Behaviour of the non-linear optical material $KTiOPO_4$ in the temperature range 293-973 K

studied by x-ray diffractometry at high resolution: alkaline displacements

Behaviour of the non-linear optical material KTiOPO$_4$ in the temperature range 293–973 K studied by x-ray diffractometry at high resolution: alkaline displacements

P Delarue†, C Lecomte†, M Jannin‡, G Marnier‡ and B Menaert‡

† Laboratoire de Cristallographie et Modélisation des Matériaux Minéraux et Biologiques, LCM^{3}B UPRESA 7036, Université Henri Poincaré, Nancy I, Faculté des Sciences, BP 239, 54506 Vandoeuvre lès Nancy Cédex, France
‡ Laboratoire de Physique de l'Université de Bourgogne, LPUB UPRESA 5027, Faculté des Sciences Mirande, BP 400, 21011 Dijon Cédex, France

Abstract. The crystal structure of potassium titanyl phosphate, KTiOPO$_4$ (space group $Pna2_1$), has been refined at room temperature, at 673 K, and at 973 K, by using accurate single-crystal x-ray diffraction techniques at high resolution ($d_{min} = 0.35$ Å). The data show a large amount of anharmonic motion of the potassium ions, increasing with temperature. To describe this motion, two models are developed: a normal refinement including potassium anharmonic thermal displacement parameters, which describes the average motion of the alkaline sites, and another model in which the potassium sites are split within the harmonic approximation and the displacements of the potassium ions versus temperature are described more precisely.

M Supplementary data files are available from the article's abstract page in the online journal; see http://www.iop.org.

1. Introduction

At room temperature and pressure, potassium titanium oxide phosphate, KTiOPO$_4$ (KTP) crystallizes in the acentric $Pna2_1$ space group [1]. Two crystallographically different distorted TiO$_6$ octahedra are linked through corners, alternately *cis*- and *trans*-coordinated, to form one-dimensional chains, which are oriented along the optic *c*-axis [001] (figure 1) [2]. These Ti–O chains with alternating long and short bonds are bridged by PO$_4$ tetrahedra, forming an open framework containing channels parallel to the *c*-axis. The two potassium cations K$^+$, not symmetry related in the $Pna2_1$ phase, lying in those channels, are relatively free to migrate and to contribute to a high anisotropic ionic conductivity. At high temperature, the KTP family shows a reversible ferroelectric-to-paraelectric phase transition [3]. The Curie temperature (T_c) of KTP is close to 1218 K [3, 4], and depends on the crystal growth conditions. After this second-order phase transition, the crystal structure belongs to the centrosymmetric space group *Pnan* [5]. In this phase the titanium octahedra are centrosymmetric, and the two potassium cations K$^+$ are symmetry related via the inversion centre.

Since KTP was introduced as an interesting non-linear optical material in 1976 [6], many isostructural compounds have received considerable attention. Several groups have proposed the use of KTP in the manufacturing of optical waveguides for crystals: waveguides have been obtained by ion exchange in which monovalent ions such as rubidium, thallium, and
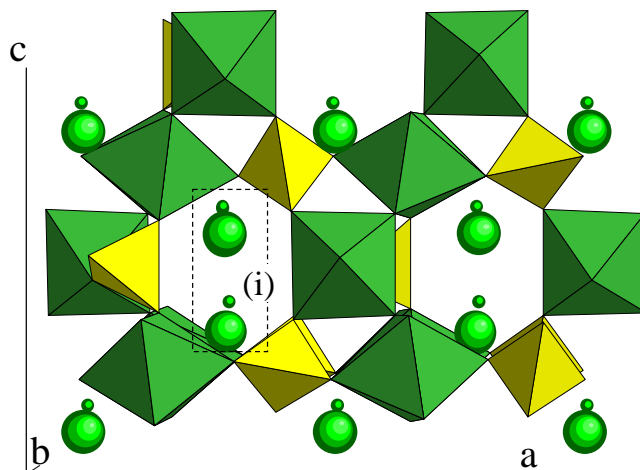
Figure 1. A view of the KTiOPO$_4$ structure, at 293 K, along the *b*-axis. The split positions for each potassium obtained at 973 K and the part of the structure (i) which enclosed the two potassium sites (K(1) and K(2)) are represented.

caesium replace the KTP potassium ions [7], or, more recently, caesium replaces the rubidium in RbTiOAsO$_4$ [8]. A precise understanding of the alkaline sites in this family would allow better control of this process. Furthermore, we have previously [9] shown that for RbTiOPO$_4$, even if the alkaline displacements have an important effect when the temperature increases, only the symmetry of the TiO$_6$/PO$_4$ framework seems to be directly correlated with the second-harmonic-generation (SHG) power.

The present work describes the variation of KTP lattice parameters, measured every 100 K from room temperature to 973 K, and the crystal structure change derived from accurate single-crystal x-ray diffraction data collected at 293, 673, and 973 K. The evolution of the structure and of its properties versus temperature is very similar to what we have observed for RbTP [9]. Then, we describe precisely the motion of the alkaline sites by using, in addition to an anharmonic refinement, a model which splits the potassium sites. This split-atom model was successfully applied to simulated and measured structure factors of RbTP [9]. Similar refinements (test and real data) were also applied by Thomas and Womersley to CsRbTA [10].

2. Data collection

The crystal was grown by the flux-growth method [11]. To reduce the problems of absorption, the sample used was ground into a sphere (diameter: 0.3 mm). Ag Kα x-ray data were collected on an Enraf-Nonius four-circle (CAD4) diffractometer at 293, 673, and 973 $\pm$ 3 K. For the high-temperature data collection, we used a locally [12] improved gas-stream heating device [13], which ensures that the crystal temperature is maintained within 3 K. Table 1 gives some experimental details of the data collection.

The temperature was increased at a rate of 3 K per minute. Every 100 K, this temperature rise was stopped and the lattice parameters determined: they were obtained by least-squares fitting to the optimized setting angles of 25 Ag Kα reflections over the range $28° < 2\theta < 38°$. After the last data collection at 973 K, during the temperature decrease, the lattice parameters were also determined by the same procedure. At each temperature, we performed successive centring procedures until the sample reached equilibrium ($\approx$2 h). The changes in the cell

Table 1. Details of data collections and refinements.

Temperature (K)	293	673	973
Specimen	Sphere radius	0.3 mm	
Lattice parameters (Å)			
a	12.807(1)	12.844(1)	12.907(2)
b	6.3981(5)	6.4245(7)	6.4609(8)
c	10.583(1)	10.579(1)	10.559(2)
$(\sin(\theta)/\lambda)_{max}$	1.39	1.39	1.39
h_{min}/h_{max}	−32/20	−32/20	−32/20
k_{min}/k_{max}	−16/16	−16/16	−16/16
l_{min}/l_{max}	−28/28	−28/28	−28/28
No of reflections measured	16712	14801	14327
No of reflections used for refinement $I > 3\sigma$	6593	5816	5685
Instrumental instability coefficient $\langle p \rangle$ [16]	2.56	2.90	2.75
R_{int}[a] (%)	2.34	2.57	2.58
Refinement program	MOLLY [19]		
The hm model			
Number of parameters	145		
Scale factor	0.3642(2)	0.3580(4)	0.3504(7)
R[b] (Rw[c]) (%)	1.79 (2.43)	2.69 (3.74)	4.42 (6.52)
Goodness of fit Z[d]	1.28	1.61	2.57
The am model			
Number of parameters	195		
Scale factor	0.3645(2)	0.3600(3)	0.3583(4)
R[b] (Rw[c]) (%)	1.58 (2.16)	1.84 (2.48)	2.68 (3.22)
Goodness of fit Z[d]	1.14	1.07	1.27
Extinction parameters[e]	1.35(2)	1.61(3)	0.35(2)
The sk model			
Number of parameters	165		
Scale factor	—	0.3604(3)	0.3589(4)
R[b] (Rw[c]) (%)	—	1.88 (2.54)	2.76 (3.39)
Goodness of fit Z[d]	—	1.09	1.34
Extinction parameters[e]	—	1.62(3)	0.34(2)
The sk model with three pairs of pseudo-atoms			
Number of parameters	185		
Scale factor	—	—	0.3592(3)
R[b] (Rw[c]) (%)	—	—	2.55 (3.07)
Goodness of fit Z[d]	—	—	1.21
Extinction parameters[e]	—	—	0.35(2)
Rogers parameter	1.06(3)	1.07(3)	1.02(4)

[a] $R_{int} = (\sum |Y - Y_{mean}|)/\sum |Y|$, the average of equivalent reflections in $mm2$ symmetry (SORTAV [17]).
[b] $R = (\sum(|F_o|-|F_c|))/\sum |F_o|$, where F_o and F_c are the observed and calculated factors respectively, w is the weight assigned to each reflection, N is the number of independent reflections, and n is the number of refined parameters.
[c] $Rw = [\sum(w(|F_o| - |F_c|)^2)/\sum w|F_o|^2]^{1/2}$.
[d] $Z = [\sum(w(|F_o| - |F_c|)^2)/(N - n)]^{1/2}$.
[e] Isotropic extinction, type 1 with Lorentzian distribution.

parameters and in the unit-cell volume versus temperature are shown in figure 2, compared to those obtained for RbTP [9]. Clearly, there is no hysteresis. We only note a slight difference between the c-values at 773 K and at 873 K. For the KTP measurements, the linear interpolations
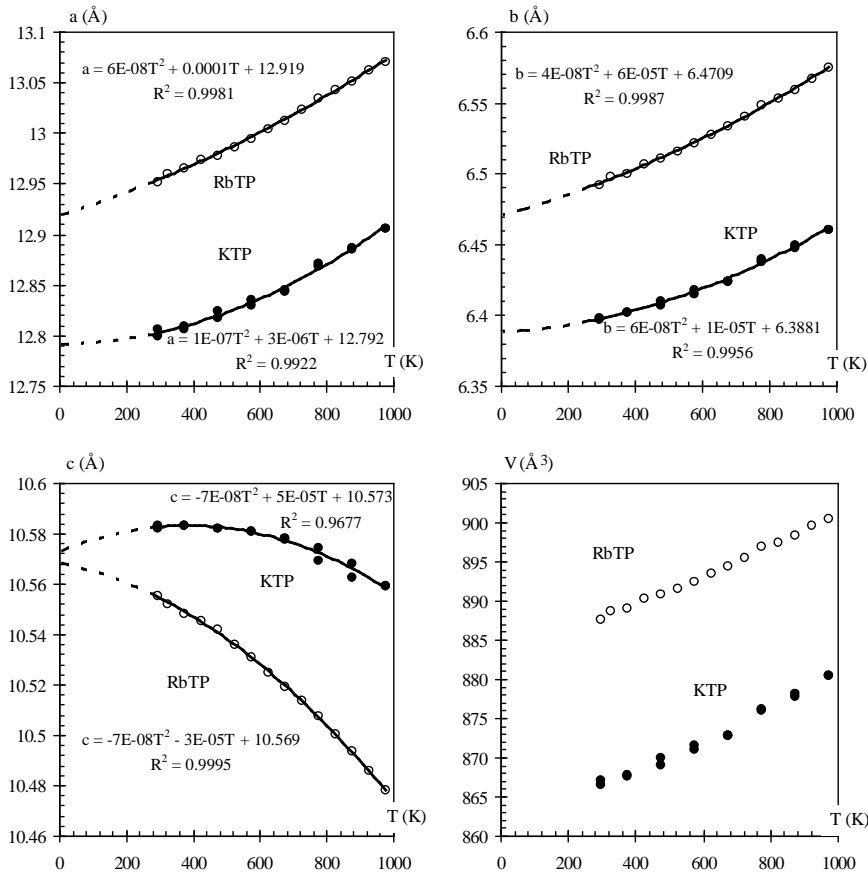
Figure 2. The evolution of the volume (Å^3) and those of the cell parameters a, b, c (Å) versus temperature (K) and quadratic fits of the data (R^2: correlation coefficient). Measurements obtained during while increasing and decreasing the temperature are shown.

Table 2. Thermal expansion coefficients (ppm K^{-1}) derived from x-ray data compared to ones derived from dilatometer data [13].

	KTP			RbTP		
	Our work	Correlation coefficient	Dilatometer data	Our work [9]	Correlation coefficient	Dilatometer data
α_{11}	12(1)	0.969	6.8	13.5(6)	0.997	10.8
α_{22}	14.7(8)	0.978	9.6	18.4(6)	0.997	13.3
α_{33}	−3.1(5)	0.831	−1.3	−10.5(3)	0.992	−5.9

give lower correlation coefficients than for RbTP (table 2). This may explain why the x-ray values are higher in magnitude (and higher than for RbTP) that those given by Chu, Bierlein, and Hunsperger [14]: the discrepancies observed between the x-ray and dilatometer data are due to the different temperature ranges. Indeed, in reference [14] the temperatures are in the range for which our results are less linear. Thus a better fit of the parameters is obtained with a quadratic form ($a_i = a_0 + \alpha_1 T + \alpha_2 T^2$), the coefficients of which are given in figure 2 together

with their correlation factors. This phenomenon is most important for the *c*-parameter, which decreases above room temperature and increases, as described by Dahaoui [15], below that temperature. This result shows that the higher anharmonic terms are stronger for KTP than for RbTP.

The data collections were performed at 293, 673, and 973 K. In order to get accurate structure factors, multiple reflections, $(h, k, \pm l)$ and $(h, -k, \pm l)$, were collected over the whole $(\sin \Theta)/\lambda$ range. Throughout the 15 days of each data collection, the maximum angular deviation, periodically controlled (every 4 h), was always less than the maximum allowed value (0.08°); owing to the use of our improved sample holder [12], no reorientation occurred. The standard intensities remained extremely stable throughout the whole experiment.

Data reduction and error analysis were performed using the DREAR programs of Blessing [16]. After background subtraction, the intensities were corrected for Lorentz and polarization effects. A polynomial fit to the slight decay of the standard reflection intensities (maximum 2.7% for $T = 673$ K) over the x-ray exposure time was applied to scale the data and to derive the instrumental instability coefficient (table 1) used in the calculation of [17]

$$\sigma^2(|F|^2) = \sigma c^2(|F|^2) + (\langle p \rangle |F|^2)^2.$$

Absorption ($\mu_{calc} = 1.65$ mm^{-1}) and beam inhomogeneity corrections were calculated by using a Blessing empirical method (SORTAV [18]): a spherical harmonic expansion in real form up to $l = 6$ for even order and $l = 3$ for odd order was found to be optimal for fitting the absorption anisotropy. The differences between the transmission factors were not significant ($A_{min} = 0.48(1)$ and $A_{max} = 0.51(1)$), and this procedure did not improve the residual factor R_{int}: for example, at room temperature, with or without corrections, the internal agreement was 2.34%. Therefore, no correction was applied to the data used for the least-squares refinements.

3. Least-squares refinements

At room temperature, the *x*-, *y*-, *z*-positions and anisotropic harmonic thermal displacement parameters U^{ij} of RbTiOPO$_4$ were used as starting parameters for the 293 K refinement using the MOLLY program [19]; to refine the structure at the other temperatures, the parameters derived from the experiment at the preceding temperature were used as the starting point. In all cases, the K atoms were refined as ions (K$^+$ scattering factors); the residual charge ($+2e$) was distributed over the ten oxygen atoms of the asymmetric unit. The core and radial valence scattering factors were calculated from Clementi wavefunctions [20]. The anomalous dispersion of each atom [21] was taken into account. For each refinement, the Rogers parameter [22] was calculated: the refined value was always close to 1.05 at each temperature (table 1); furthermore, the Flack parameter [23] ($-0.02(3)$ at room temperature) confirmed that the crystal was very close to showing a single domain of structure polarity. Like in our previous work on RbTP [9], we used three refinement models to consider the thermal displacement parameters of the K$^+$ ions.

3.1. The harmonic (hm) model

The *x*-, *y*-, *z*-positions and the anisotropic thermal displacement parameters U^{ij} of all of the atoms were obtained from the usual harmonic thermal motion refinement. For room temperature data, as shown in table 1 (the hm model), the agreement indices R, Rw, Z are excellent. But these values rise with temperature, and the residual density calculated at
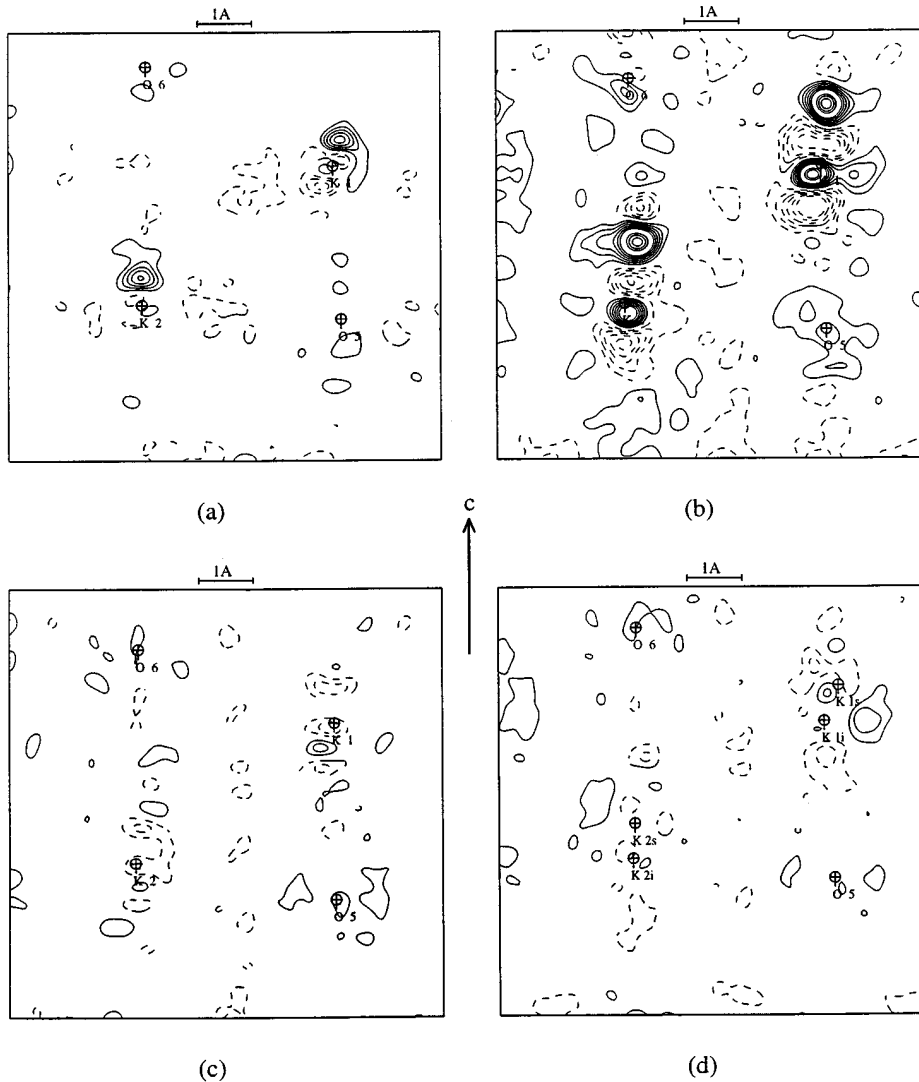
Figure 3. The residual density in the plane defined by K(1)(x, y, z), K(2) and K(1)$(x, y, 1 + z)$: the harmonic (hm) model at 293 K (a), and at 973 K (b); the anharmonic (am) model at 973 K (c); and the split-atom (sk) model at 973 K (d). The contour intervals are at 0.2 electrons Å^{-3}; negative contours are dashed curves and zero contours are omitted.

experimental resolution (see $((\sin\theta)/\lambda)_{max}$ in table 1)

$$\Delta^{res}\rho(\vec{r}) = \frac{1}{V}\sum_{\vec{H}}[k^{-1}|F_o(\vec{H})| - |F_c(\vec{H})|]\exp(\mathrm{i}[\varphi_c(\vec{H}) - 2\pi\vec{H}\cdot\vec{r}])$$

(where F_o and F_c are respectively the observed and calculated structure factors, and φ_c is the phase of the calculated structure factor) around the K sites increased a lot with increasing temperature (figures 3(a) and 3(b)). The high-temperature maps show without any doubt that the harmonic model is not applicable to alkaline ions. Hence, in the following, two other K$^+$ thermal motion models are used.

3.2. The anharmonic (am) model

The harmonic Debye–Waller factor $T_0(\vec{H})$ was corrected by using the Gram–Charlier series expansion, which is a Taylor-series-like expansion using the rectilinear Gaussian probability density function and its successive derivatives [24]. As programmed in MOLLY [19], the thermal anharmonic factor $T(\vec{H})$ becomes

$$T(\vec{H}) = T_0(\vec{H})\left[1 + \frac{i^3}{3!}C^{jkl}h_jh_kh_l + \frac{i^4}{4!}D^{jklm}h_jh_kh_lh_m + \cdots\right]$$

(where C^{jkl} and D^{jklm} are the third- and the fourth-order Gram–Charlier coefficients respectively.)

At room temperature, the residual $R(F)$ factors are 1.79, 1.58, 1.58, and 1.57% after refinements up to the second-, fourth-, fifth-, and sixth-order Gram–Charlier coefficients for the alkaline sites, respectively. To reduce the number of parameters to a minimum and to facilitate comparison of the changes of the structure at various temperatures, the K atoms were anharmonically refined only up to the fourth-order Gram–Charlier coefficients for every temperature. On this hypothesis, the minimum observations/parameters ratio is 29 (table 1). In spite of the high correlation coefficients (>0.80) for the second-order $T_0(\vec{H})$ and the fourth or third orders, the amplitudes of some anharmonic coefficients are very significant, and their values increase with temperature. The most important terms ($>20\sigma$) are: at 293 K, C^{333} (K(1)) and C^{333} (K(2)); at 673 K, C^{333} (K(1)), C^{133} (K(1)), and C^{333} (K(2)); and at 973 K, C^{333} (K(1)), D^{3333} (K(1)), D^{1333} (K(1)), D^{2333} (K(1)), C^{333} (K(2)), and D^{3333} (K(2)). The anharmonic coefficients are more important in magnitude in the c-direction and for site 1 than for site 2. This model significantly improved the fit (table 1); however, if the residual-electron-density peak heights around K sites calculated with the anharmonic refinements are smaller than those obtained with the hm model, some peaks still exist (figure 3(c)) especially at 973 K.

Within this am model hypothesis, figure 4 gives the evolution of the thermal displacement parameters. For Ti, P, and O, the average value of U_{eq} for each type of atom ($U_{eq} = (U^{11} + U^{22} + U^{33})/3$) is linear versus temperature, and the straight line passes through the origin (figure 4(a)). This is not the case for K⁺. The evolutions of the thermal coefficients U^{ij} of K(1) and K(2) are similar (figure 4(b)): only the linear fitting for U^{33} does not intercept the origin. At 0 K, its value is negative, which is physically wrong, in the harmonic approximation. Despite a refinement at the fourth order of the Gram–Charlier coefficients for K⁺, modelling each K⁺ ion by a single site is not adequate. As for RbTP, it needs a more sophisticated model which splits the K⁺ ions onto two sites elongated along the c-axis. The distance between these two atom sites must decrease to zero at 0 K.

3.3. Splitting K sites (the sk model)

In this model, each potassium-ion site has been split into two independent parts; the sum of the multiplicities of the two sets of pseudo-atoms was constrained to be 1 during all refinements. At 293 K, we observed too short a distance between the two K⁺ positions at each K(1) and K(2) site, leading to a too strong correlation between their x-, y-, z-, U^{ij}-, and occupancy parameters. Therefore, at room temperature, in order to compare the results with higher-temperature ones, the harmonic (hm) model will be used. At 673 K, x, y, z, and U^{ij} calculated from the am model were used as starting parameters. For each K⁺ ion, two pseudo-atoms, identified by the labels ip and sp, were originally located at the sites x_K, y_K, z_K with multiplicities of 0.5 and 0.5 respectively. During the refinement process, these two atoms split naturally, with different occupancies, towards different positions (K(1, ip), K(1, sp) for site 1 and K(2, ip) and K(2, sp) for site 2, corresponding respectively to the initial room temperature position, ip, and
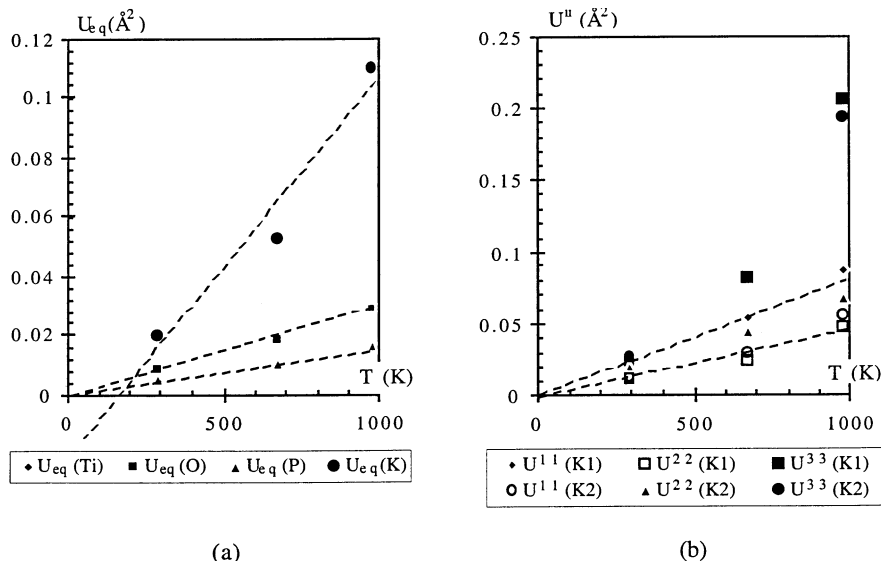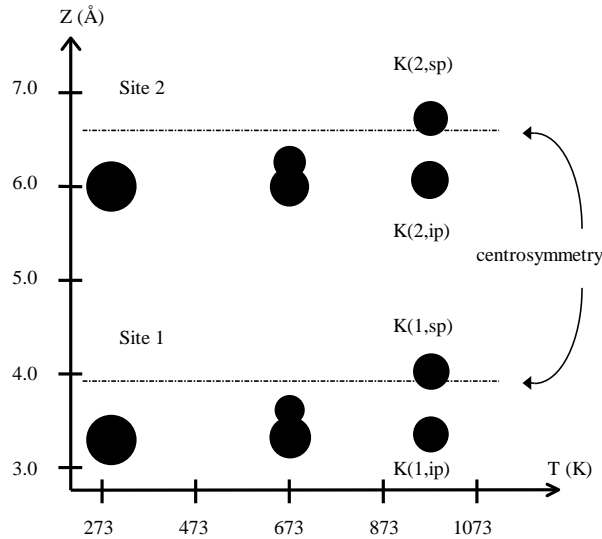
Figure 4. The evolution of the average value of the thermal motion U_{eq} ($U_{eq} = (U^{11}+U^{22}+U^{33})/3$) (the am model) for each type of atom (Å^2) (a) (the points for Ti and P are superimposed on the scale of this diagram), and the evolution of U^{ii} for each K(1) and K(2) site (Å^2) (b), versus temperature (K).

to the high-temperature-split position, sp). At $T = 673$ K, at the end of the refinement, the distances between the two pseudo-atom sites were 0.298(5) and 0.260(4) Å along the c-axis for K(1) and K(2) respectively. At 973 K the same procedure of refinement was applied. The resulting distances between the sites are 0.67(1) and 0.65(1) Å along the c-axis for K(1) and K(2) respectively. When the temperature increases, the multiplicity of ip sites decreases in favour of that of sp sites, and converges to 0.5.

For both high-temperature refinements, despite some correlation (>0.85) between the K pseudo-atom parameters due to the small distances, this split-atom model improved the fit significantly (table 1). Figure 5 gives the evolutions for these two pseudo-atoms at each site along the c-axis versus the temperature.

This model is not totally satisfactory. The evolution versus temperature of the average thermal displacement parameters U_{eq} of the K ions is more linear and the extrapolated value at 0 K is closer to the origin than for the anharmonic model—but it is not completely linear and the intercept does not really pass through the origin (figure 6(a)). Figure 6(b) gives the evolution of these parameters for each pseudo-atom, which shows that the non-harmonicity of the thermal motion is mainly that of the sp sites (K(1, sp) and K(2, sp)). Moreover, the residual-electron-density map at 973 K (figure 3(d)) still shows positive and negative peaks, principally around alkaline site 1.

Thus, to improve this model for KTP at 973 K, we split the sp model sites into two new independent sites, leading now to three pseudo-atoms for each alkaline ion: K(1, ip), K(1, sp′), and K(1, sp″) for site 1, and K(2, ip), K(2, sp′), and K(2, sp″) for site 2. The refinement process used was similar to that applied previously. The three pairs of pseudo-atoms (K(1, α) and K(2, α) with $\alpha = $ ip, sp′, or sp″) were refined alternatively, due to the high correlation (>0.85) between the K pseudo-atom parameters. The fit to the structure factors was improved significantly. With fewer parameters than in the am model refinement (185 parameters instead

Figure 5. The evolution of the potassium sites (see (i) in figure 1) obtained with the two-atom-split (sk) model, versus temperature (K). The distances are represented along the *c*-axis, and the surfaces of the disc are proportional to the occupancy of each pseudo-site.

(a)

(b)
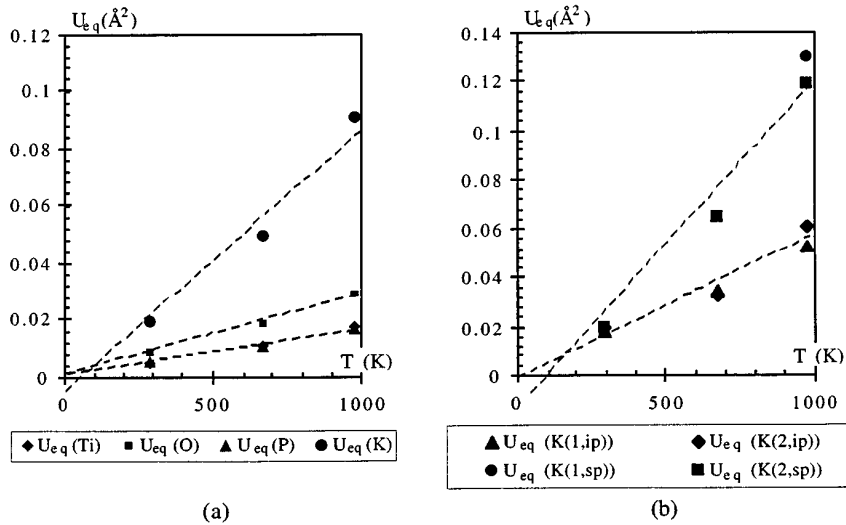
Figure 6. The evolution of the average value of the thermal motion U_{eq} ($U_{eq} = (U^{11}+U^{22}+U^{33})/3$) (the sk model) for each type of atom (Å^2) (a) (the points for Ti and P are superimposed on the scale of this diagram), and the evolution of U_{eq} for each pseudo-atom at the two potassium sites (Å^2) (b), versus temperature (K).

of 195), the residual factor obtained ($R = 2.55$ at 973 K) is lower than that found for the anharmonic model (table 1). The positional and thermal parameters for these pseudo-atoms are given in table 3.

The positional, thermal, and occupancy parameters obtained, at each temperature, with the am and the sk models are given in the supplementary material.

Table 3. Positional, equivalent thermal, and occupancy parameters obtained at 973 K with the splitting of K sites (the sk model) in the case of three pseudo-atoms at each site.

| | Fractional coordinates ($\times 10^4$) | | | | |
	x	y	z	U_{eq} (10^4 Å^2)	Occupancy ($\times 10^3$)
K(1, ip)	3780(1)	7777(2)	3176(1)	550(8)	511(4)
K(2, ip)	1083(1)	7145(4)	665(2)	424(10)	314(6)
K(1, sp′)	4099(6)	8229(12)	3752(16)	1431(57)	187(7)
K(2, sp′)	1023(4)	6867(10)	913(11)	851(25)	388(7)
K(1, sp″)	3880(3)	7843(5)	3855(19)	1048(51)	298(0)
K(2, sp″)	1099(3)	7073(4)	1507(13)	1078(42)	297(0)

4. Discussion and conclusions

For KTP, at room temperature, Thomas and Glazer [25] showed that there are hole sites (h(1) and h(2)) related by pseudosymmetry to the inequivalent potassium sites K(1) and K(2). They deduced that the ionic diffusion paths for K$^+$ along [001] involve both potassiums and hole sites (K(1)–h(2)–K(2)–h(1)–K(1)). As expected from our previous RbTP measurements [9], the major effect of the temperature on KTP over the temperature range studied is the displacement of the K ions along the c-axis. The split-atom model shows that the initial room temperature position, ip, does not change for any K ion, and that its occupancy decreases in favour of the sp sites, which move in the $+c$-direction to produce a global high-temperature centrosymmetric structure (figure 5). Then the sp sites converge to the centrosymmetric positions (the centre of symmetry is (1/4, 1/4, 1/4) for the high-temperature phase) of the initial positions (ip) corresponding to the hole sites. As for RbTP [9], this confirms the ionic paths proposed by Thomas and Glazer [25]. In the same way, it has been observed that ion exchange of Rb in KTP is more efficient (deeper and more rapid) on the $-c$-face than on the $+c$-face [26]. The ion-exchange process is enhanced by the presence of a large number of vacancies in the crystal. The K$^+$ ions move more readily, by the ionic path proposed, towards the $-Z$-surface; thus the exchange process is expected to be more efficient at this end of the crystal. This physical reason for this difference between $+Z$ and $-Z$ given by Thomas and Glazer [25] is also confirmed by our results.

The magnitudes of the anharmonic coefficients are higher for alkaline site 1 than for alkaline site 2. The maps at 973 K (figures 3(c) and 3(d)) show more residual-density peaks around alkaline site 1. Thus, whatever the model, the thermal motions of the two K sites are not similar. Site 1 shows more anharmonic thermal motion. Both K ions occupy large cavities enclosed by the oxygen framework. K(2) is coordinated by nine oxygen atoms. As K(1) and K(2) are symmetry related via the inversion centre at high temperature, for the sake of comparison we consider the nine nearest oxygen neighbours for K(1). In that case, at room temperature, the shortest and longest bond are respectively K(1)–O(3) = 2.713(1) Å and K(1)–O(6) = 3.518(1) Å for site 1, and K(2)–O(1) = 2.677(1) Å and K(2)–O(4) = 3.108(1) Å for site 2. Thus, the K(1) free volume appears more distorted than the K(2) one. This could explain the thermal motion differences of the sites.

On the other hand, comparison of KTP and NaTiOPO$_4$ at 110 K [27] shows that Na ions have more freedom to vibrate. In the same way, at room temperature, the average alkaline–oxygen bond lengths of the two sites are 2.925(1) and 2.993(1) Å for KTP and RbTP respectively. This increase of 2.3% (when the rubidium ions replace the potassium ions) is smaller than the increase of the ionic radius, which is 6.1% ($r(K^+)$ = 1.65 Å and $r(Rb^+)$ = 1.75 Å [28]). This may explain why the split-atom model, which gives excellent

results for the study of RbTP, is not totally satisfactory for KTP. The thermal motion of the sp sites in KTP is more extensive than that in RbTP. Thus the K ions, which are smaller than Rb ions, are less easily positioned in cavities. A further study of the electrostatic potential based on x-ray data or a one-particle potential (opp) [29] may give more information on the sp-site evolution.

In conclusion, the two models fit the data equally well: the anharmonic model describes the average motion of the potassium ions; also it gives global information concerning the distinct behaviours of the alkaline sites. But the split-atom model, which gives excellent results for RbTP [9], goes a little further: it gives more precise information on the K-ion displacement versus temperature, even if this model is not totally satisfactory for the present study of KTP.

Due to technical limitations, and also because KTP would certainly melt at around T_c, it was not possible to study the KTP phase transition and its centrosymmetric phase as Belokoneva *et al* did for germanate analogues of the KTP structure [30]. The same type of study was also performed by Favard *et al* for ASbSiO$_4$ (A = Na, K) and ASbOGeO$_4$ (A = Rb, K) [31]. In these studies, where the centrosymmetric phase was found to exist, the x-ray data were also fitted via a split-atom model. However, even if the centrosymmetric phase was not reached in the present study, it is possible to draw the following conclusion: like for RbTP [9], the divergence from centrosymmetry of the structure or of the TiO$_6$/PO$_4$ framework only may be calculated with the program Missym [32]. The evolution versus temperature of the TiO$_6$/PO$_4$ framework divergence is very similar to the evolution of the SHG intensity [3] measured for KTP (figure 7). We plan to measure the SHG coefficients as functions of T for a single crystal, to determine more precisely the correlation between the evolution of the structure and the SHG properties.
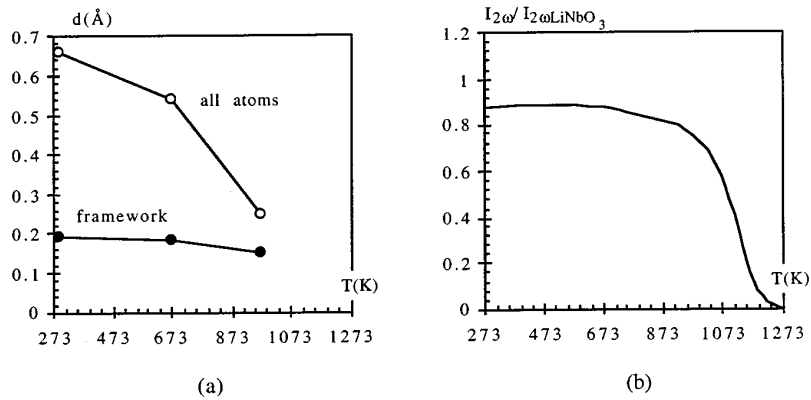
Figure 7. (a) The evolution of the distance (Å) from the average position of the pseudosymmetry plane or inversion centre, considering all of the structure or only the TiO$_6$/PO$_4$ framework, versus temperature (K). (b) The temperature (K) dependence of the second-harmonic-generation intensity $I_{2\omega}$ measured for KTiOPO$_4$ [3].

Acknowledgments

References

[1] Masse R and Grenier J C 1971 *Bull. Soc. Fr. Minéral. Cristallogr.* **94** 437
[2] Tordjman I, Masse R and Guitel J C 1974 *Z. Kristallogr.* **139** 103
[3] Yanovskii V K and Voronkova V I 1986 *Phys. Status Solidi* a **93** 665
[4] Chu D K T, Hsiung H, Cheng L K and Bierlein J D 1993 *IEEE Trans. Ultrason., Ferroelectr., Freq. Control* **40** 819
[5] Harrison W T A, Gier T E, Stucky G D and Schultz A J 1995 *Mater. Res. Bull.* **30** 1341
[6] Zumsteg F C, Bierlein J D and Gier T E 1976 *J. Appl. Phys.* **47** 4980
[7] Bierlein J D, Ferretti A, Brixner and L H and Hsu W Y 1987 *Appl. Phys. Lett.* **50** 1216
[8] Hu Z W, Thomas P A and Risk W P 1998 *Phys. Rev.* B **58** 6074
Womersley M N, Thomas P A and Corker D L 1998 *Acta Crystallogr.* B **54** 635
[9] Delarue P, Lecomte C, Jannin M, Marnier G and Menaert B 1998 *Phys. Rev.* B **58** 5287
[10] Thomas P A and Womersley M N 1998 *Acta Crystallogr.* B **54** 645
[11] Marnier G, Boulanger B, Menaert B and Metzger M 1988 *Fr Patent Specification* FR 2609976
[12] Delarue P and Jannin M 1999 *J. Appl. Crystallogr.* at press
[13] Argoud R and Capponi J J 1984 *J. Appl. Crystallogr.* **17** 420
[14] Chu D K T, Bierlein J D and Hunsperger R G 1992 *IEEE Trans. Ultrason., Ferroelectr., Freq. Control* **39** 683
[15] Dahaoui S 1996 *PhD Thesis* University of Nancy I, France
[16] Blessing R H 1987 *Crystallogr. Rev.* **1** 3
[17] McCandlish L E, Stout G H and Andrews L C 1975 *Acta Crystallogr.* A **31** 245
[18] Blessing R H 1995 *Acta Crystallogr.* A **51** 33 and references therein
[19] Hansen N K and Coppens P 1978 *Acta Crystallogr.* A **34** 909
Hansen N K 1983 *MOLLY: Aspherical Pseudo-Atom Refinement on X-ray Diffraction Data* LCM^{3}B, University Henry Poincaré, Nancy I, France
[20] Clementi E 1965 *IBM J. Res. Dev. (Suppl.)* **9** 2
[21] Maslen E N, Fox A G and O'Keefe M A 1992 *International Tables for X-ray Crystallography* vol C, ed A J C Wilson (Dordrecht: Kluwer) p 219
[22] Rogers D 1981 *Acta Crystallogr.* A **37** 734
[23] Flack H D 1983 *Acta Crystallogr.* A **39** 876
[24] Ibers J A and Hamilton W C 1974 *International Tables for X-ray Crystallography* vol 4 (Birmingham: Kynoch)
[25] Thomas P A and Glazer A M 1991 *J. Appl. Crystallogr.* **24** 968
[26] Van der Poel C J, Bierlein J D, Brown J B and Colak S 1980 *Appl. Phys. Lett.* **57** 2074
[27] Dahaoui S, Hansen N K and Menaert B 1997 *Acta Crystallogr.* C **53** 1173
[28] Shannon R D 1976 *Acta Crystallogr.* A **32** 751
[29] Bachmann R and Schultz H 1984 *Acta Crystallogr.* A **40** 668
[30] Belokoneva E L, Knight K S, David W I F and Mill B V 1997 *J. Phys.: Condens. Matter* **9** 3833
[31] Favard J F, Verbaere A, Piffard Y and Tournoux M 1994 *Eur. J. Solid State Inorg. Chem.* **31** 995
[32] Le Page Y 1988 *J. Appl. Crystallogr.* **21** 983